Use of Prussian Blue pseudocapacitive properties to amplify the pulsed amperometric readout of biosensors

Guagneli, Luca; Supala, Eszter; Palomaki, Tommi; Perez, Alejandro Garcia; Haeggstrom, Edward; Bobacka, Johan

Published in:
Biosensors and Bioelectronics

DOI:
10.1016/j.bios.2025.118283

Published: 01/03/2026

Document Version
Final published version

Document License
CC BY

Biosensors and Bioelectronics 295 (2026) 118283

Contents lists available at ScienceDirect

Biosensors and Bioelectronics

journal homepage: www.elsevier.com/locate/bios

Use of Prussian Blue pseudocapacitive properties to amplify the pulsed amperometric readout of biosensors

Luca Guagneli [a], Eszter Supala [a], Tommi Palomäki [a], Alejandro García Pérez [a], Edward Hæggström [a], Johan Bobacka [a,b,*]

[a] GlucoModicum Ltd, Toinen linja 7, 00530, Helsinki, Finland
[b] Åbo Akademi University, Faculty of Science and Engineering, Johan Gadolin Process Chemistry Centre, Laboratory of Molecular Science and Engineering, Henriksgatan 2, 20500, Turku/Åbo, Finland

ARTICLE INFO

Keywords:
Glucose biosensor
Prussian Blue
Hydrogen peroxide detection
Pulsed amperometry
Wearable glucose biosensor
Continuous glucose monitoring

ABSTRACT

Enzymatic electrochemical biosensors are a cornerstone technology in enabling further advancements in the field of Continuous Glucose Monitoring (CGM). Pulsed amperometric methods improve the sensitivity and accuracy of electrochemical biosensors. The literature shows that pulsed amperometry increases the sensitivity of enzymatic glucose biosensors based on Prussian Blue (PB). However, the underlying mechanism responsible for this improvement is poorly understood, which impedes further development of this promising measurement method. The present work elucidates the role of the spontaneous reaction between hydrogen peroxide (H_2O_2) and Prussian White (PW) in the sensitivity improvement observed with pulsed amperometry. A charged working electrode (WE) containing PW can catalyze the H_2O_2 reduction in the open-circuit regime (OCP). The consumption of H_2O_2 over a 30-min contact at OCP was 65 % at a PW WE, compared to 13 % at a PB WE. This spontaneous process is associated with a partial discharge of the WE (PW → PB) between the amperometric pulses. The subsequent re-charging (PB → PW) yields the current amplification observed with pulsed amperometry. Based on this consideration, we developed and validated a model for glucose quantification using pulsed amperometry that considers the spontaneous reaction of H_2O_2 with PW. The model achieves 0.998 determination coefficient between glucose concentration and four analytical signals. The insights presented in this work support the optimization and development of the pulsed amperometric detection method in enzymatic glucose biosensors. Additionally, this work advances the understanding of H_2O_2 detection at PB-based sensors, and contributes to the development of precise and accurate enzymatic glucose biosensors.

1. Introduction

Diabetes is a leading medical condition of the 21st century, projected to affect 850 million people worldwide by 2050 ("Diabetes around the world in 2024, Fact sheets," n.d.). Continuous Glucose Monitoring (CGM) is a cornerstone technology in the management and prevention of diabetes. CGM provides continuous real-time data on glucose levels and offers a viable alternative to traditional intermittent glycemic control methods. CGM systems give people with diabetes the opportunity to make informed decisions on their lifestyle and improve their health, to mitigate the risk of disease-related complications and reduce the need for medical care (Chesser et al., 2024; Choe et al., 2022; Schubert-Olesen et al., 2022; Lin et al., 2021). Current CGM systems still face issues related to affordability, precision, and limited wear time. To overcome these challenges and to promote a broader adoption of CGM, further research and developments in the field of electrochemical biosensors are fundamental.

Electrochemical biosensors are widely used in wearable devices for CGM due to their high sensitivity and selectivity, fast response, low detection limit, and cost effectiveness. Furthermore, biosensors offer versatility to analyze different body fluids. Prussian Blue (PB) has emerged as an advantageous electroactive material for voltammetric and coulometric enzymatic glucose biosensors (Fu et al., 2025; Li et al., 2022; Ying et al., 2021). The widespread use of PB as electrode material for wearable glucose biosensors is due to its simple and versatile synthesis, chemical stability, biocompatibility, and high selectivity. Moreover, the advantageous electrocatalytic properties of PB allow hydrogen peroxide reduction at a potential close to 0.0 V *vs.* Ag/AgCl, and

* Corresponding author. GlucoModicum Ltd, Toinen linja 7, 00530, Helsinki, Finland.
E-mail address: johan.bobacka@abo.fi (J. Bobacka).

https://doi.org/10.1016/j.bios.2025.118283
Received 7 August 2025; Received in revised form 22 November 2025; Accepted 30 November 2025
Available online 1 December 2025

therefore minimize the effect of interfering redox compounds (Karyakin, 2017; Jia et al., 2010; Ricci and Palleschi, 2005).

The scientific research in the field of amperometric and coulometric biosensors is focused on the use of micro- and nano-structured materials (Crapnell and Banks, 2021; Welch et al., 2021; Chu et al., 2017), enzymatic layer structuring and immobilization (Dong et al., 2025; Prabhakar et al., 2025; Gupta et al., 2022), and integration of microfluidic systems (Fattahi and Hasanzadeh, 2022; Schmidt-Speicher and Länge, 2021). However, the analytical methods used to detect the analyte receive insufficient attention. The analytical methods directly influence the sensitivity and accuracy of the biosensors. In amperometric methods, the biosensor sensitivity can be substantially increased by using pulsed amperometric methods. Pulsed Amperometric Detection (PAD) (Trojanowicz, 2011; LaCourse and Modi, 2005) is an established method in voltammetric analyzers of flow systems, *e.g.*, in gas or liquid chromatography.

In recent reports, pulsed amperometry was employed in a PB-based glucose biosensor and validated *in vivo*. Pulsed amperometry provided 100x increase in sensitivity and 15x increase in the signal-to-background ratio compared to continuous amperometry (Komkova et al., 2023). The highest sensitivity was obtained with a short readout time (20 ms) after applying the potential. The authors suggested that the open-circuit intervals between the amperometric pulses allow for analyte replenishment within the diffusion layer (Komkova et al., 2023, 2025). However, this interpretation overlooks the important contribution of the continuous and spontaneous analyte consumption and the pseudocapacitive properties of PB. A charged PB WE, where the mediator is mainly in the PW form, retains its ability to catalyze the reduction of H_2O_2 in open-circuit conditions. Overlooking these contributions hinders the possibility of optimizing the pulsed amperometric method to achieve maximal sensitivity and accuracy. Both are key requirements for applications in wearable devices involving minute (nanoliter) sample volumes.

Our present study sets out to demonstrate that the enhanced current obtained with the pulsed amperometric method in PB-based glucose biosensors is due to the spontaneous process between H_2O_2 and PW. The reduction of H_2O_2 continues in the open-circuit regime, and causes a partial discharge of the WE between the amperometric pulses. Moreover, this study demonstrates that the current enhancement does not rely on the replenishment of the diffusion layer. This finding is used to develop a model of glucose detection in PB-based enzymatic biosensors with pulsed amperometry. Based on this model, the biosensor and the measurement method can be optimized to achieve increased current amplification. A deeper understanding of the interaction between the analyte and the mediator enables and supports further method optimization, and allows achieving improved biosensor performance. This work also provides critical insights into the detection of H_2O_2 in PB-based sensors, which contributes to the further development of precise and accurate glucose biosensors for glucose monitoring in wearable devices.

2. Materials and methods

2.1. Chemicals and reagents

All chemicals were used as received from the listed suppliers, if not otherwise specified. Deionized water (resistivity = 18.2 MΩ cm) was prepared with a Barnstead Pacific TII water purification unit (Thermo Fisher Scientific, USA). Phosphate buffered saline (PBS) pouches (Merck, Germany) were dissolved in deionized water to obtain a 10 mM phosphate buffered solution of 137 mM NaCl and 2.7 mM KCl with pH 7.4. Potassium chloride, glycerol, glucose oxidase (GOx, from *Aspergillus niger*), peroxidase from horseradish (HRP), poly(ethylene glycol) diglycidyl ether (PEGDE), D(+)-glucose and dimethyl sulfoxide were purchased from Merck. Hydrogen peroxide (H_2O_2, 30 wt% in water) and Amplex™ Red reagent were obtained from Thermo Fisher Scientific. A commercially available 10 % TGX Stain-Free FastCast Kit (BioRad, USA) was used to prepare the polyacrylamide (PAG) interface.

2.2. Biosensor preparation

The working electrode (WE) consisted of a screen-printed layer of carbon and Prussian Blue on top of a conductive carbon layer (diameter 9 mm). The counter and reference electrodes (CE and RE) consisted of screen-printed Ag and AgCl. The sensors were obtained from Screentec (Finland). The sensors were used as received, without surface treatment prior to enzyme deposition. The WE was functionalized by drop-casting a solution containing GOx immobilized with poly(ethylene glycol) diglycidyl ether (PEGDE) following a protocol adapted from (Vasylieva et al., 2011). The biosensors used for glucose detection were coated with a hydrogel based on PAG, fully hydrated in PBS. The hydrogel film covered the WE, CE, and RE. The effect of the presence of the hydrogel layer has been described in (Kemp et al., 2022).

2.3. Equipment

Cyclic voltammograms (CV) were recorded with a MultiPalmSens4 potentiostat (PalmSens, The Netherlands). Pre-treatment steps were applied with a MultiPalmSens4 potentiostat. Chronoamperometric curves were recorded using a proprietary device incorporating a commercially available AD5940 potentiostat (Analog Devices, USA) or using the MultiPalmSens4. The OCP measurements were performed with the AD5940 potentiostat or a Digital Multimeter 34465A (Keysight technologies, USA). The fluorometric analysis of H_2O_2 was done with a Varioskan LUX plate reader (Thermo Scientific).

2.4. Methods

The CVs were recorded using screen-printed bare carbon-PB electrodes, *i.e.*, sensors without enzyme and a hydrogel coating on WE, CE, and RE. The supporting electrolyte was 0.1 M KCl or PBS. The CVs were recorded in the potential range from −0.4 to +0.6 V, at a scan rate of 50 mV/s, with a potential step of 5 mV, for 10 cycles.

The glucose calibrations were performed in the concentration range 5–100 μM (in PBS), in an increasing concentration order. 88 μL of PBS was added on top of the hydrogel which acted as a thin electrochemical cell and prevented the hydrogel from drying. The sampling rate of chronoamperometric and OCP measurements was 100 ms. The current signals were integrated following the trapezoidal rule to obtain the charge values. Statistical analyses were performed with OriginLab 2023 software.

The spontaneous reduction of H_2O_2 at the WE was investigated using bare screen-printed carbon-PB electrodes. PBS was added on the WE, RE, and CE to act as electrochemical cell. First, a pre-treatment step was performed by applying 0.0 V or +0.4 V for 15 min on the WE to set the electrochemical state of the mediator. In a parallel experiment, no pre-treatment was involved in the protocol. Then, H_2O_2 was added to the electrochemical cell, and an OCP or a chronoamperometric measurement at 0.0 V was started. The total volume of the H_2O_2 solution was 400 μL. Aliquots of 10 μL were collected after given time intervals, and their H_2O_2 concentration was determined with a fluorometric method using Amplex™ Red reagent after the experiment. The plate reader first injected HRP to each well, then recorded the fluorescence every 30 s for 10 min at 600 nm emission wavelength (excitation: 571 nm, 12 nm bandwidth). The H_2O_2 concentration was calculated from the final values using a standard calibration curve.

2.5. Pulsed amperometry

In pulsed amperometry, the amperometric measurement is divided into cycles of a set of subsequent steps. The applied potential is switched between different values (Fig. 1a), or alternatively, the WE is kept at

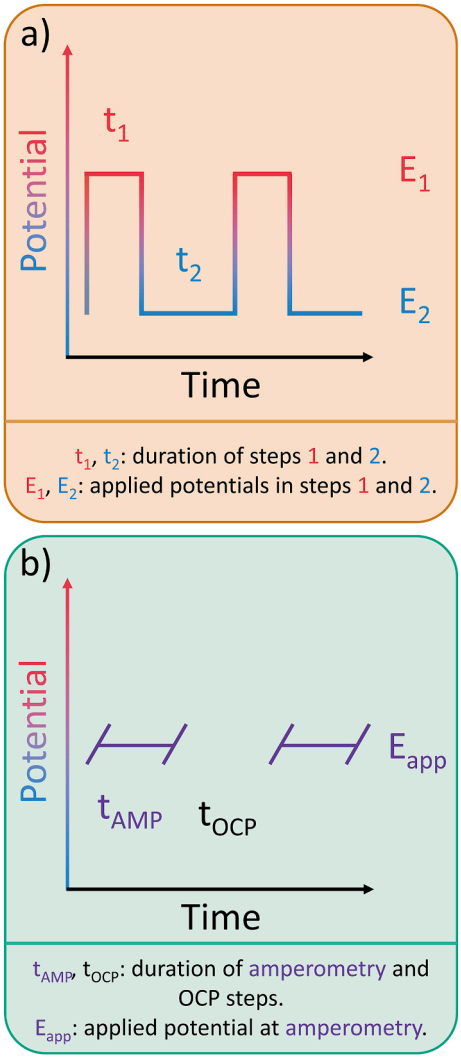

Fig. 1. Schematic graph of the measurement methods used in pulsed amperometry: a) multi-potential step waveform (here: double-potential), and b) applied potential steps with intermittent pauses at OCP. In this work type b) was used with E_{app} = 0.0 V vs. Ag/AgCl (140 mM Cl^- in PBS).

OCP between the amperometric steps (Fig. 1b). The first approach is suitable for systems where faradaic processes take place at the surface of the WE (*e.g.*, detection at noble metal electrodes), and the latter one is relevant for materials with higher pseudocapacitance. The pulsed amperometric method used in this work is based on the one proposed for PB-based biosensors to detect glucose (Komkova et al., 2023). It comprises repeated cycles of amperometry (AMP) at an applied bias potential of 0.0 V and OCP measurement. The pulsed amperometric method used in this work employs a sequence of cycles of t_{AMP} = 10 s and t_{OCP} = 15 s.

3. Results and discussion

This work demonstrates that the spontaneous reduction of H_2O_2 at a charged PB-based WE in the open-circuit regime (at OCP) is the main contributor to the current amplification observed using the pulsed amperometry method to detect glucose. The experimental results presented and discussed in the following sections confirm and describe the spontaneous reduction of H_2O_2 at OCP at a charged PB-based WE. Determination coefficients R^2 = 0.998 between the glucose concentration and four analytical signals are consistent with the contribution of the spontaneous reduction of H_2O_2 at OCP. Moreover, the results confirm that the analyte is consumed at the same rate with the pulsed and continuous methods, and indicate a lack of a major replenishment of the H_2O_2 diffusion layer. These results contradict the hypothesis that the replenishment of the diffusion layer is the main contributor to the current amplification observed with pulsed amperometry. These findings provide critical insights into the H_2O_2 detection at a PB WE, contribute to the further development of the pulsed amperometric method and support the development of precise and accurate PB-based enzymatic glucose biosensors.

3.1. Spontaneous reduction of H_2O_2 by PW in the absence of applied bias potential

The experimental data presented in this section support the hypothesis that the reduction of H_2O_2 proceeds spontaneously at a PB-based WE in absence of an applied potential.

The experimental data in Fig. 2 shows the evolution of the concentration of H_2O_2 over 30 min at a PB electrode at different potentials. Pre-treatment steps were run before introducing H_2O_2. The pre-treatment steps set the redox state of the mediator in the WE to its PB ($Fe_4^{III}[Fe^{II}(CN)_6]_3$) or PW ($K_4Fe_4^{II}[Fe^{II}(CN)_6]_3$) form before introducing H_2O_2. A commonly used bias potential for PB-based H_2O_2 sensors is 0.0 V *vs.* Ag/AgCl. The CV provided in Fig. S1 shows that 0.0 V *vs.* Ag/AgCl (PBS electrolyte, 140 mM Cl^-) is close to the reduction peak of the PB/PW redox couple. Therefore, upon application of 0.0 V, the WE is charged, and the equilibrium between PB and PW is shifted towards PW (Karyakin, 2001) according to Eq (1):

$$PB + 4e^- + 4K^+ \leftrightarrows PW \quad (1)$$

In contrast, a pre-treatment at +0.4 V drives the equilibrium of PB/PW towards PB. H_2O_2 is added after the pre-treatment, and it diffuses towards the WE surface where it reacts with the mediator. PW has high selectivity and electrochemical activity towards H_2O_2 (Karyakin, 2017). Due to the ability of H_2O_2 to insert into the mediator lattice (Itaya et al., 1984), H_2O_2 is reduced (Ricci and Palleschi, 2005; Karyakin et al., 1999) according to Eq (2):

$$H_2O_2 + 2e^- \rightarrow 2OH^- \quad (2)$$

The reduction of H_2O_2 occurs together with the oxidation of PW to PB according to Eq (3):

$$PW + 2H_2O_2 \rightarrow PB + 4\,OH^- + 4K^+ \quad (3)$$

After the pre-treatment step, a continuous chronoamperometry measurement at 0.0 V or an open-circuit potential (OCP) measurement was run during the 30-min contact time with the H_2O_2 solution. The results in Fig. 2 show that 65.0 % of the H_2O_2 is reduced in the OCP regime after 30 min at a WE driven to a high PW/PB ratio (Fig. 2a). As a comparison, only 13.4 % of H_2O_2 is reduced in the OCP regime when the WE is driven to a high PB/PW ratio (Fig. 2c). This is attributed to a spontaneous process that proceeds in absence of the applied bias potential (*i.e.*, at OCP), when PW is available on the WE surface. The average consumption rates of H_2O_2 after pre-treatment at 0.0 V (Fig. 2a) were compared. During the first 5 min of the chronoamperometry and OCP measurement, the consumption rates were 0.97 and 0.95 μM/min, respectively. This suggests that during the first minutes of the OCP regime, the spontaneous process proceeds at the same rate as during the amperometric measurement, and therefore, that the H_2O_2 diffusion layer does not replenish at OCP. Moreover, Fig. 2d indicates that without an electrochemical pre-treatment at 0.0 V, the mediator in the WE is mostly in its oxidized form (PB), which is due to the oxygen in the atmosphere upon storage.

The spontaneous reduction of H_2O_2 in the absence of bias potential is explained with the PB electrochemical properties. PB and Prussian Blue Analogues (PBAs) are used in energy storage and electrochemical separation methods due to their ability to intercalate and retain certain ions

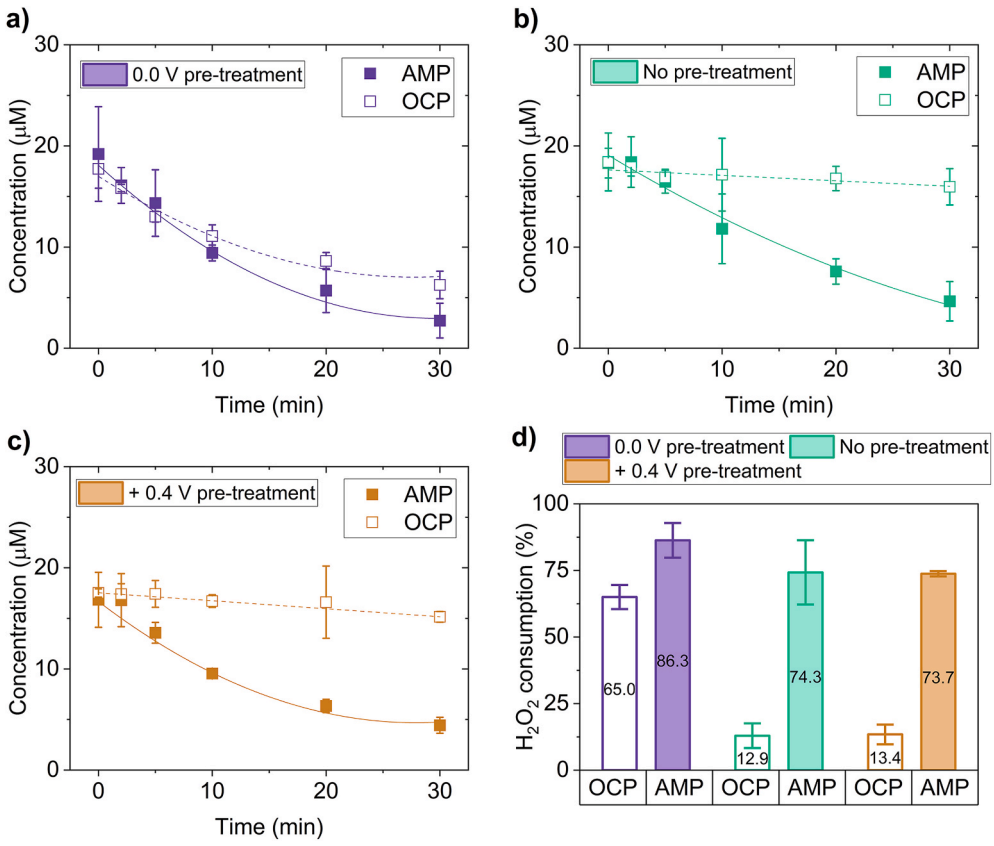

Fig. 2. Change in the H_2O_2 concentration during a 30-min contact of the solution with the WE, containing PB/PW a) after a 15-min pre-treatment step at 0.0 V, b) with no pre-treatment, and c) after a 15-min pre-treatment at +0.4 V. After the pre-treatment step, chronoamperometry at 0.0 V (full squares, AMP) or OCP measurement (empty squares) was conducted. The data are represented as average ± SD, n = 3. Trend lines are added for readability. d) Consumption (%) of H_2O_2 after 30 min of contact obtained from the data presented in a-c.

while undergoing reversible faradaic redox processes (Jiang et al., 2022; Qiu et al., 2022; Su and Hatton, 2017). PW retains its redox state and its ability to undergo faradaic processes in the presence of an active analyte, even after the bias potential is removed, due to its pseudocapacitive properties. Hence, the reduction of H_2O_2 continues as a spontaneous process at the WE in absence of any applied bias potential (*i.e.*, at OCP). The reduction of H_2O_2 causes a partial discharge of the WE, *i.e.*, a partial oxidation of PW to PB. Therefore, the discharge rate of the WE depends on the concentration of H_2O_2. This will be discussed in the following section.

3.2. *Pulsed amperometric detection of glucose with the spontaneous reduction of H_2O_2*

In a glucose biosensor based on GOx, glucose reacts with the enzyme to produce H_2O_2 (Bankar et al., 2009):

$$\beta - D - Glucose + O_2 \xrightarrow{GOx} H_2O_2 + \beta - D - Gluconolactone \quad (4)$$

H_2O_2 reacts with PW at the WE surface and produces PB according to Eq (3). Upon application of a constant bias potential, the produced PB is immediately reduced back to PW according to Eq (1). The ratio of PB/PW remains constant over time. Hence, during a continuous amperometric measurement, the source of the amperometric current is the continuous H_2O_2 reduction. In contrast, in the pulsed amperometric

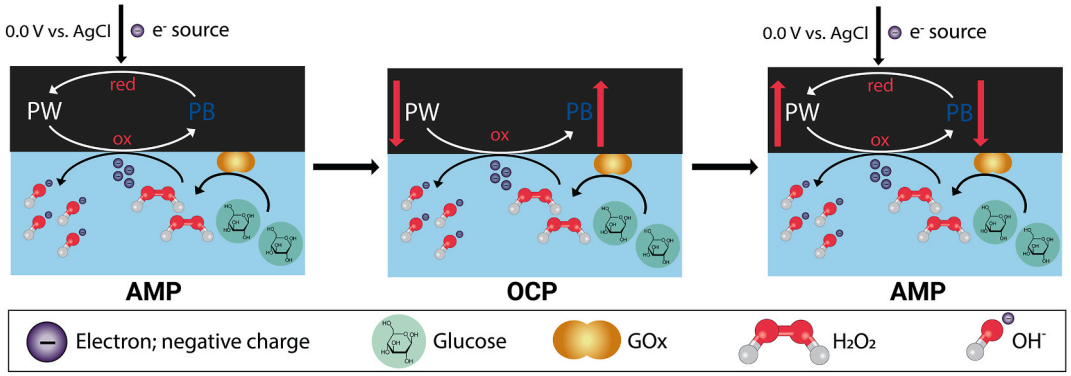

Fig. 3. Proposed mechanism of pulsed amperometry using PB as mediator. The red arrows indicate an increase or a decrease in the amount of PB and PW.

method, H_2O_2 is reduced spontaneously during the OCP steps, as shown in Fig. 3. This causes the oxidation of PW to PB according to Eq (3), and leads to a partial discharge of the WE. The PB/PW ratio increases, and the OCP is expected to increase.

As long as the OCP remains close to 0.0 V, the reduction of H_2O_2 proceeds in absence of an applied potential. Therefore, the development of the diffusion layer is not affected by the measurement step (OCP or amperometry). The H_2O_2 reduction rate drives the rate of oxidation of PW to PB as well as the rate of the OCP increase. Upon application of the bias potential, the WE is charged to its equilibrium state at 0.0 V. The ratio of PB/PW is forced to its equilibrium at 0.0 V, and all the PW that was oxidized to PB during the OCP step is reduced back to PW. The reduction current originating from this process, together with the ongoing reduction of H_2O_2 during amperometry, and the charging current due to the potential step to 0.0 V, determine the signal measured at the WE.

A typical biosensor response during glucose calibration with the pulsed amperometric method is shown in Fig. S2. Fig. 4 shows calibration plots that were obtained by plotting the current, charge, and the average slope of an entire OCP signal versus the glucose concentration.

The concentration range was chosen to reflect the intended clinical application of the glucose biosensor. The 5–100 μM range is necessary for non-invasive glucose monitoring applications. Such range is a requisite for direct analysis of glucose in sweat (Cheong et al., 2025; Tang et al., 2024), and is necessary for applications where sub-microliter sample volumes of interstitial fluid are extracted and diluted into the electrolyte of an interface layer (Kemp et al., 2022; Hakala et al., 2022). The biosensors yielded a linear response in the tested concentration range of 5–100 μM. The linear regression analyses of all the selected analytical signals resulted in R^2 values up to 0.998. This indicates high correlation with the glucose concentration and supports the proposed model. Based on the mechanism shown in Fig. 3 and the results of Fig. 4 it can be concluded that:

a) the current value at the beginning of the amperometric signal correlates with the amount of PW that is oxidized to PB during the previous OCP step;
b) the current value at the end of the amperometric signal correlates more closely with the steady-state rate of the H_2O_2 reduction;
c) the charge calculated from a full amperometric pulse correlates with the amount of H_2O_2 reduced at the WE during the previous OCP step and the given amperometric pulse;
d) the slope of the OCP signal between the amperometry steps correlates with the average reaction rate during the OCP step. The instantaneous derivative correlates with the steady-state reaction rate.

In practice, this means that the sensitivity, in terms of current and charge vs. glucose concentration, increases with increasing duration of the OCP step (t_{OCP}) in presence of glucose, and agrees with the

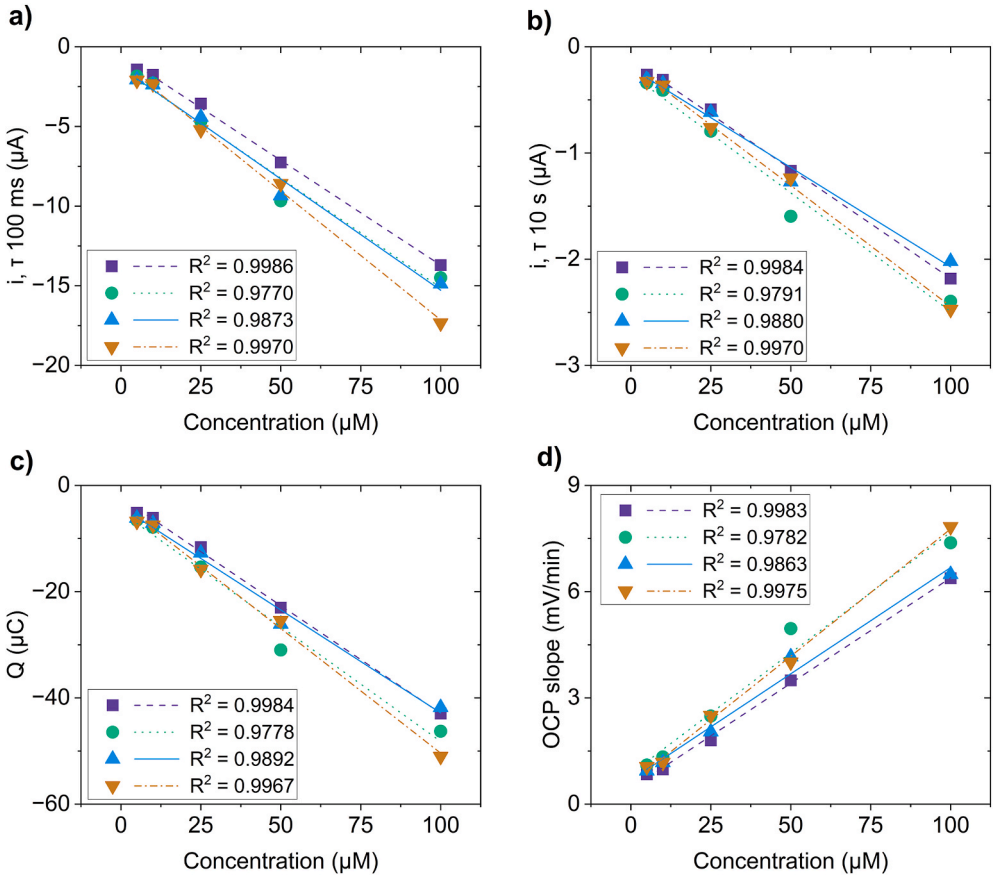

Fig. 4. Linear correlation plots between the glucose concentration and different analytical signals of pulsed amperometry (t_{OCP} = 15 s and t_{AMP} = 10 s), where each color represents datapoints from one biosensor. Each glucose addition increases the amount of H_2O_2 produced and being reduced at the WE, and hence results in more negative amperometric signals (see Fig. S2). The amperometric pulses used for the data analysis correspond to the peak signals with the most negative current after each glucose addition. The OCP signals used for the data analysis correspond to the OCP measurements immediately before the above-mentioned peak amperometric signals. The datasets were obtained as follows: a) current at sampling time τ = 100 ms, corresponding to the beginning of the amperometric signal, b) current at sampling time τ = 10 s, corresponding to the end of the amperometric signal, c) charge integrated in the time window 0–10 s of the peak amperometric signal, d) average slope of the entire OCP signal in the time window 0–15 s (before the next peak amperometric signal). The R^2 values of the calibration lines of each dataset are provided in the graphs.

sensitivity increase reported in (Komkova et al., 2023). When t_{OCP} = 15 s, the biosensors achieved an average sensitivity of 0.22 μA/(μM cm^2) using the amperometric signal recorded at 100 ms after OCP (Fig. 4a), and 0.67 μC/(μM cm^2) using the charge of a full amperometric pulse (Fig. 4c). The LOD was 9 μM (3.3σ/s). The biosensors achieved superior performance compared to recently presented biosensor designs for non-invasive glucose monitoring applications (Table S1). For further information regarding sensitivity, LOD and RMSD values (Root Mean Square Deviation), the reader is referred to Table S2, Table S3, and Table S4, respectively. Response times, and prediction and confidence bands (95 % confidence level) of the cumulative datasets can be found from Fig. S3 and Fig. S4, respectively.

As shown in Fig. 4d, the H_2O_2 concentration determines the rate of OCP increase, which is due to the partial discharge of the WE (*i.e.*, the oxidation of PW to PB). The sensitivity in terms of the OCP slope was 0.10 mV/(min μM cm^2). Therefore, the detection of glucose using a PB-based enzymatic biosensor can be carried out also in a chronopotentiometric mode. In this case, the potential drift serves as the analytical signal, and the application of a bias potential acts as a step to restore the ratio between PB and PW. Similar approaches using biosensors, where a chronopotentiometric method provides the analytical signal and a discharging step is added to the measurement protocol, have been proposed for measuring glucose and other analytes (Lee et al., 2019, 2022; Kinyua Muthuri et al., 2021).

Selectivity is a critical parameter in enzymatic biosensors for glucose determination. Species such as ascorbic acid, uric acid, and acetaminophen, are known interferents in *in vivo* glucose monitoring applications (Bellido et al., 2023; Pullano et al., 2022; Jia et al., 2010). However, the low potential applied to reduce H_2O_2 at a PB electrode minimizes the effect of such interferents (Karyakin, 2017; Jia et al., 2010; Ricci and Palleschi, 2005). The scope of this investigation is to elucidate the mechanism of glucose detection with pulsed amperometry, while an interference study is an important topic of future research.

3.3. Consumption of glucose – continuous vs. pulsed amperometry

Fig. S5 shows typical response curves of a biosensor with pulsed and continuous amperometric methods with subsequent additions of the same amount of glucose. Fig. 5 shows a comparison of the current (*i*) and charge (*Q*) values measured with additions of the same amount of glucose with the pulsed and continuous amperometric methods. The pulsed amperometric method increased the amplitude of the peak of the electric current. However, the total charge measured at the WE remained the same as in continuous amperometry. Hence, the amount of H_2O_2 that is reduced at the WE is the same with the two methods. This result confirms that the method used to detect the analyte does not affect the consumption of the analyte itself. Equal consumption of the analyte with continuous and pulsed amperometry further suggests the presence of a spontaneous reduction of H_2O_2 during the OCP steps of the pulsed amperometric method.

3.4. Charge of the amperometric pulses as a function of the OCP

When using pulsed amperometry to detect glucose, the rate of OCP increase depends on the amount of PW that is oxidized to PB as H_2O_2 is reduced in open-circuit conditions. Hence, the OCP value right before the amperometry (the pre-amperometry OCP) depends on the glucose concentration. Fig. 6a shows an extract from a glucose calibration, where an addition of glucose causes a gradual increase of the pre-amperometry OCP and the amperometric current.

Using a different approach, the PB/PW ratio can be tuned with a pre-treatment step prior to the amperometric pulses. The OCP of the biosensor after the pre-treatment step corresponds to the pre-treatment potential, and it depends on the PB/PW ratio. Pre-treatment steps at potentials in the range of +0.5 to +3.0 mV were used to set the pre-amperometry OCP in absence of glucose. The amperometric response

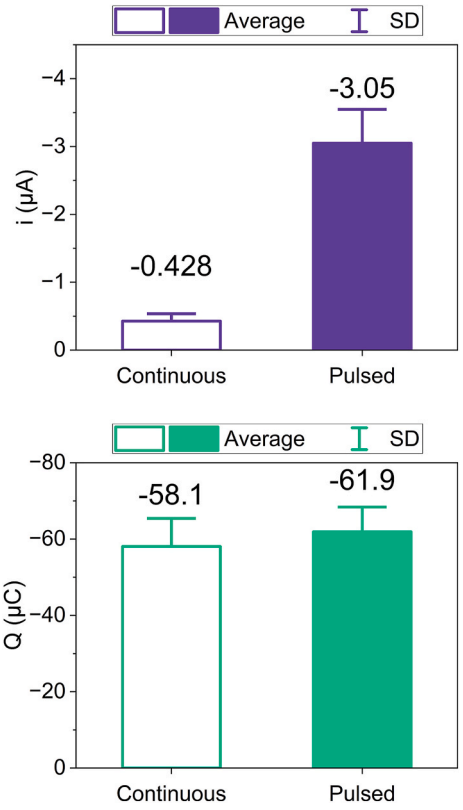

Fig. 5. Comparison of the analytical signals obtained from additions of equal amount of glucose with continuous (empty bars) and pulsed (full bars, t_{OCP} = 15 s and t_{AMP} = 10 s) amperometric methods. In the continuous amperometry set, the current values (purple, empty bar) correspond to the peak current after the glucose additions. In the pulsed amperometry set, the current values (purple, full bar) correspond to the current at sampling time τ = 100 ms of the negative peak amperometric signal after the glucose additions. The charge values (green) are obtained by integrating the current signal in a time window of 5 min after the glucose addition (equivalent to 12 pulses in the pulsed method). The baseline signal, acquired before the additions, is subtracted from the datapoints. The bars represent average ± SD (n = 12).

was recorded at 0.0 V after the pre-treatment. Examples of amperometric pulses after pre-treatment at +1, +2.5, +0.5, and +3.0 mV are shown in Fig. 6b.

During the amperometry steps PB is reduced to PW and a current is produced. The integral of the current yields a charge, that in presence of H_2O_2, includes the charge that is accumulated due to the oxidation of PW to PB by H_2O_2 in open-circuit conditions. Fig. 6c shows that the charge values correlate linearly with the pre-amperometry OCP. The ratio between the charge and the OCP depends on the capacitance of the WE. The correlation is present both with and without glucose. The correlation was used to compare the charge generated in the case where a) the pre-amperometry OCP is reached with the spontaneous reduction of H_2O_2 in open-circuit conditions in presence of glucose, with the case where b) the pre-amperometry OCP is set with the electrochemical pre-treatment in absence of glucose. Fig. 6c shows that the biosensors generate similar charge values in the two abovementioned cases. The minor difference between the two datasets can be explained considering that H_2O_2 is reduced during both the OCP and the amperometric steps. This resulted in increased charge values in presence of H_2O_2 compared to the case where H_2O_2 is absent (for a given pre-amperometry OCP).

The results indicate that biosensors where the pre-amperometry OCP is reached by the spontaneous reduction of H_2O_2 or other processes (*e.g.*, electrochemical pre-treatment or O_2 reduction at PW), produce comparable total amounts of charge in the amperometric pulse. This behavior is consistent with the hypothesis that the charge measured

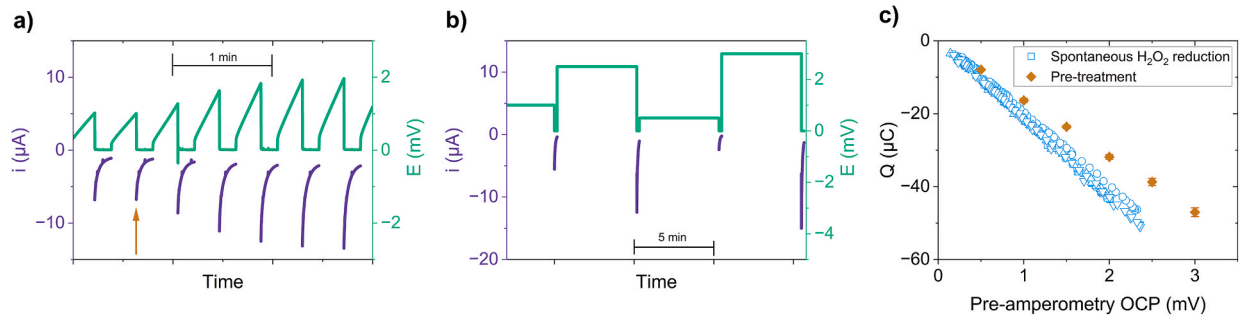

Fig. 6. a) Section of a glucose calibration recorded with the pulsed amperometry method (t_{OCP} = 15 s and t_{AMP} = 10 s). The arrow indicates a glucose addition. b) Applied potential (green) during a set of 5-min pre-treatment steps, and subsequent amperometric pulses recorded at 0.0 V (t_{AMP} = 10 s, purple curves). c) The integrated charge values from the time window 0–10 s of single amperometric pulses vs. the pre-amperometry OCP values during glucose calibration (blue symbols, glucose concentration range 5–100 μM) or after the pre-treatment at different bias potentials in the absence of glucose (brown symbols). The brown datapoints are presented as average ± SD, n = 9 (3 points from 3 biosensors), while the blue datapoints represent one biosensor per symbol type.

during the amperometric pulse corresponds to the oxidation of PB to PW, rather than to the reduction of the analyte. A biosensor where H_2O_2 replenishes the diffusion layer during the OCP step would generate more charge than a biosensor without glucose, as it implies that the H_2O_2 reduction starts when the bias voltage is applied. Therefore, these results indicate that H_2O_2 is reduced during the OCP step, and it does not replenish the diffusion layer. The replenishment of the diffusion layer is not the main contributor to the current amplification observed with pulsed amperometry.

3.5. Implications for further development of the pulsed amperometric measurement method

The hypothesis of replenishment of the diffusion layer implies that, in pulsed amperometry, the diffusion properties of H_2O_2 limit the ability to amplify the electric current. However, this is not the case when considering the contribution of the spontaneous reduction of H_2O_2. Instead, the biosensor design and measurement parameters can be optimized to increase the sensitivity obtained with the pulsed amperometric method.

According to the interpretation of the results of this work, the parameters that affect the magnitude of the sensor response are:

- The amount of mediator available to react with H_2O_2: a charged WE that contains more PW (more mediator) enables the spontaneous reduction of more H_2O_2. More PW (*e.g.,* larger electrode geometric area) allows storing more charge. This increases the current amplification during the following amperometric step.
- Duration of OCP steps: a longer OCP step permits more H_2O_2 to be reduced spontaneously at the WE. This increases the current amplification in the following amperometric step if coupled with a higher amount of mediator. This spontaneous process between PW and H_2O_2 occurs probably on the WE surface, and it is followed by a charge distribution in the bulk of the PB/PW mediator layer. The spontaneous reaction proceeds as long as there is PW available, and within an OCP range where the WE is active towards the H_2O_2 reduction.
- Duration of the amperometric pulses: a longer amperometric pulse allows the reduction of all the newly generated PB to PW, and therefore the return to the original equilibrium ratio, indicated by an OCP close to the bias potential. This also ensures that there is enough PW available for the spontaneous reaction during the next OCP step.
- Bias potential: setting a sufficiently low bias potential ensures that there is enough PW available for the spontaneous reaction during the OCP step.

4. Conclusions

We investigated the mechanism of glucose detection with pulsed amperometry at a PB-based enzymatic biosensor. We demonstrated the role of the spontaneous reduction of H_2O_2 at OCP in the current amplification improvement observed with pulsed amperometry. The spontaneous reduction of H_2O_2 at OCP causes the oxidation of PW to PB, and leads to a partial discharge of the WE between the amperometric pulses. The current originating from the re-charging of the WE (reduction of PB to PW) during the amperometric step is the analytical signal measured in the pulsed amperometric detection of glucose. This study contradicts the hypothesis that the replenishment of the diffusion layer is the main contributor to the current amplification observed with pulsed amperometry.

We demonstrated that a charged working electrode containing PW catalyzes the H_2O_2 reduction in absence of applied potential (*i.e.*, at OCP). Over a 30-min contact at OCP, 65 % of H_2O_2 was reduced at a PW WE, compared to only 13 % at PB WE. The average H_2O_2 consumption rates during chronoamperometry and at OCP at a PW WE were 0.97 and 0.95 μM/min, respectively (t = 5 min).

We validated our proposed model of the pulsed amperometric detection of glucose that considers the spontaneous reduction of H_2O_2. Determination coefficients R^2 = 0.998 between the glucose concentration and four analytical signals indicate the contribution of the spontaneous process. The biosensors achieved an average sensitivity of 0.22 μA/(μM cm^2) and 0.67 μC/(μM cm^2), LOD = 9 μM. Pulsed amperometry allows the glucose detection in chronopotentiometric mode, using the slope of the OCP as the analytical signal, with a sensitivity of 0.10 mV/(min μM cm^2). We presented evidence that glucose is consumed at the same rate with the pulsed and continuous amperometric methods.

This work presents insights that enable further development of the pulsed amperometric measurement method. The enzymatic conversion of glucose and the reduction of H_2O_2 at the surface of a charged PB WE start soon after the glucose addition, already before applying a bias potential for the readout. This affects the recovery rate of the biosensor, especially when the biosensor is used to measure minute (nanoliter) sample amounts in wearable device applications. These insights are broadly applicable to H_2O_2 detection at PB-based enzymatic biosensors, and are expected to be valid for the detection of other analytes. Therefore, this work contributes to the development of precise and accurate wearable devices for monitoring of glucose and other analytes.

An extensive clinical performance study is in progress. The study is conducted with a complete system for the determination of glucose in interstitial fluid extracted from humans. This clinical study serves to validate our wearable and non-invasive glucose sensing system for real use, including studies of potential interferents. This investigation is a large endeavor that will be published separately.

CRediT authorship contribution statement

Luca Guagneli: Writing – review & editing, Writing – original draft, Visualization, Methodology, Investigation, Formal analysis, Conceptualization. **Eszter Supala:** Writing – review & editing, Visualization, Methodology, Investigation, Formal analysis, Conceptualization. **Tommi Palomäki:** Writing – review & editing, Supervision, Project administration, Conceptualization. **Alejandro García Pérez:** Writing – review & editing, Supervision. **Edward Hæggström:** Writing – review & editing. **Johan Bobacka:** Writing – review & editing, Supervision, Conceptualization.

Funding sources

The work carried out in this project was fully funded by GlucoModicum Ltd.

Declaration of competing interest

We declare that the manuscript is only submitted to Biosensors and Bioelectronics.

The manuscript is not under consideration for publication elsewhere, its publication is approved by all authors, by the Board of GlucoModicum Ltd., where the work was carried out, and, if accepted, it will not be published elsewhere in the same form, in English or in any other language, including electronically without the written consent of the copyright-holder.

A.G.P, E.H., and J.B. are co-founders of GlucoModicum Ltd, which develops technologies and products for needle-free health and biomarker monitoring and holds patents related to the sampling method based on magnetohydrodynamics (MHD). L.G., E.S., A.G.P., T.P., E.H, and J.B. are employees of GlucoModicum Ltd. E.H and J.B. are scientific advisors to GlucoModicum Ltd. and board members of GlucoModicum Ltd.

Acknowledgements

The authors acknowledge the support of Risto Vänskä for presenting material that inspired this work. The authors acknowledge the support of the technical laboratory staff of GlucoModicum Ltd who participated in the preparation of the materials used in this work. In particular, the authors acknowledge the support of Alaska Timilsina and Heini Laine in the data acquisition throughout the project that delineated the work published in this article. The authors acknowledge the support of the feedback received from the R&D staff of GlucoModicum Ltd throughout the project. The authors acknowledge the support of Omar Escalante for the help in preparing the graphical material.

Appendix A. Supplementary data

Supplementary data to this article can be found online at https://doi.org/10.1016/j.bios.2025.118283.

Data availability

Data will be made available on request.

References

Bankar, S.B., Bule, M.V., Singhal, R.S., Ananthanarayan, L., 2009. Glucose oxidase — an overview. Biotechnol. Adv. 27, 489–501. https://doi.org/10.1016/j.biotechadv.2009.04.003.

Bellido, V., Freckman, G., Pérez, A., Galindo, R.J., 2023. Accuracy and potential interferences of continuous glucose monitoring sensors in the hospital. Endocr. Pract 29, 919–927. https://doi.org/10.1016/j.eprac.2023.06.007.

Cheong, S., Chae, J., Lee, H., Hong, S.H., Lim, H., Bae, H., Lee, K., Shin, S., Kim, T.Y., Hahn, S.K., 2025. Microfluidic tesla valve sweat patch integrated smartwatch for optical continuous monitoring of glucose, oxygen, and heart rate. Biosens. Bioelectron. 289, 117925. https://doi.org/10.1016/j.bios.2025.117925.

Chesser, H., Srinivasan, S., Puckett, C., Gitelman, S.E., Wong, J.C., 2024. Real-time continuous glucose monitoring in adolescents and young adults with type 2 diabetes can improve quality of life. J. Diabetes Sci. Technol. 18, 911–919. https://doi.org/10.1177/19322968221139873.

Choe, H.J., Rhee, E.-J., Won, J.C., Park, K.S., Lee, W.-Y., Cho, Y.M., 2022. Effects of patient-driven lifestyle modification using intermittently scanned continuous glucose monitoring in patients with type 2 diabetes: results from the randomized open-label PDF study. Diabetes Care 45, 2224–2230. https://doi.org/10.2337/dc22-0764.

Chu, Z., Liu, Y., Jin, W., 2017. Recent progress in Prussian blue films: methods used to control regular nanostructures for electrochemical biosensing applications. Biosens. Bioelectron. 96, 17–25. https://doi.org/10.1016/j.bios.2017.04.036.

Crapnell, R.D., Banks, C.E., 2021. Electroanalytical overview: utilising micro- and nano-dimensional sized materials in electrochemical-based biosensing platforms. Microchim. Acta 188, 268. https://doi.org/10.1007/s00604-021-04913-y.

Diabetes around the world in 2024, Fact sheets, n.d. . Int. Diabetes Fed. Atlas. URL https://diabetesatlas.org/resources/factsheets/(accessed 7.February.2025).

Dong, X., Qi, Y., Wang, Z., 2025. A review of enzyme immobilization technology in continuous glucose monitoring systems. Front. Chem. Sci. Eng. 19, 1–17. https://doi.org/10.1007/s11705-025-2554-1.

Fattahi, Z., Hasanzadeh, M., 2022. Nanotechnology-assisted microfluidic systems for chemical sensing, biosensing, and bioanalysis. TrAC, Trends Anal. Chem. 152, 116637. https://doi.org/10.1016/j.trac.2022.116637.

Gupta, U., Gupta, V., Arun, R.K., Chanda, N., 2022. Recent advances in enzymatic biosensors for point-of-care detection of biomolecules. Biotechnol. Bioeng. 119, 3393–3407. https://doi.org/10.1002/bit.28251.

Hakala, T.A., Zschaechner, L.K., Vänskä, R.T., Nurminen, T.A., Wardale, M., Morina, J., Boeva, Z.A., Saukkonen, R., Alakoskela, J.-M., Pettersson-Fernholm, K., Hæggström, E., Bobacka, J., García Pérez, A., 2022. Pilot study in human healthy volunteers on the use of magnetohydrodynamics in needle-free continuous glucose monitoring. Sci. Rep. 12, 18318. https://doi.org/10.1038/s41598-022-21424-9.

Itaya, K., Shoji, N., Uchida, I., 1984. Catalysis of the reduction of molecular oxygen to water at Prussian blue modified electrodes. J. Am. Chem. Soc. 106, 3423–3429. https://doi.org/10.1021/ja00324a007.

Jia, W.-Z., Wang, K., Xia, X.-H., 2010. Elimination of electrochemical interferences in glucose biosensors. TrAC, Trends Anal. Chem. 29, 306–318. https://doi.org/10.1016/j.trac.2010.01.006.

Jiang, M., Hou, Z., Ren, L., Zhang, Y., Wang, J.-G., 2022. Prussian blue and its analogues for aqueous energy storage: from fundamentals to advanced devices. Energy Storage Mater. 50, 618–640. https://doi.org/10.1016/j.ensm.2022.06.006.

Karyakin, A.A., 2017. Advances of Prussian blue and its analogues in (bio)sensors. Curr. Opin. Electrochem. 5, 92–98. https://doi.org/10.1016/j.coelec.2017.07.006.

Karyakin, A.A., 2001. Prussian blue and its analogues: electrochemistry and analytical applications. Electroanalysis 13, 813–819. https://doi.org/10.1002/1521-4109(200106)13:10<813::AID-ELAN813>3.0.CO;2-Z.

Karyakin, A.A., Karyakina, E.E., Gorton, L., 1999. On the mechanism of H2O2 reduction at prussian blue modified electrodes. Electrochem. Commun. 1, 78–82. https://doi.org/10.1016/S1388-2481(99)00010-7.

Kemp, E., Palomäki, T., Ruuth, I.A., Boeva, Z.A., Nurminen, T.A., Vänskä, R.T., Zschaechner, L.K., Pérez, A.G., Hakala, T.A., Wardale, M., Haeggström, E., Bobacka, J., 2022. Influence of enzyme immobilization and skin-sensor interface on non-invasive glucose determination from interstitial fluid obtained by magnetohydrodynamic extraction. Biosens. Bioelectron. 206, 114123. https://doi.org/10.1016/j.bios.2022.114123.

Kinyua Muthuri, L., Nagy, L., Nagy, G., 2021. Chronopotentiometric method for assessing antioxidant activity: a reagentless measuring technique. Electrochem. Commun. 122, 106907. https://doi.org/10.1016/j.elecom.2020.106907.

Komkova, M.A., Kasimovskaya, V.S., Eliseev, Artem A., Poyarkov, A.A., Sushkov, A.I., Eliseev, Andrei A., Karyakin, A.A., 2025. Pulse-operated first-generation biosensors with extended linear range for continuous glycemia monitoring in oxygen-deficient environments. Anal. Chem. 97, 18928–18935. https://doi.org/10.1021/acs.analchem.5c01058.

Komkova, M.A., Eliseev, Artem A., Kasimovskaya, V.S., Poyarkov, A.A., Eliseev, Andrei A., Karyakin, A.A., 2023. Pulse power generation chronoamperometry as an advanced readout for (Bio)sensors: application for noninvasive diabetes monitoring. Anal. Chem. 95, 7528–7535. https://doi.org/10.1021/acs.analchem.2c05746.

LaCourse, W.R., Modi, S.J., 2005. Microelectrode applications of pulsed electrochemical detection. Electroanalysis 17, 1141–1152. https://doi.org/10.1002/elan.200403233.

Lee, I., Loew, N., Tsugawa, W., Ikebukuro, K., Sode, K., 2019. Development of a third-generation glucose sensor based on the open circuit potential for continuous glucose monitoring. Biosens. Bioelectron. 124–125, 216–223. https://doi.org/10.1016/j.bios.2018.09.099.

Lee, I., Wakako, T., Ikebukuro, K., Sode, K., 2022. In vitro continuous 3 months operation of direct electron transfer type open circuit potential based glucose sensor: heralding the next CGM sensor. J. Diabetes Sci. Technol. 16, 1107–1113. https://doi.org/10.1177/19322968221092449.

Lin, R., Brown, F., James, S., Jones, J., Ekinci, E., 2021. Continuous glucose monitoring: a review of the evidence in type 1 and 2 diabetes mellitus. Diabet. Med. 38, e14528. https://doi.org/10.1111/dme.14528.

Prabhakar, T., Giaretta, J., Zulli, R., Rath, R.J., Farajikhah, S., Talebian, S., Dehghani, F., 2025. Covalent immobilization: a review from an enzyme perspective. Chem. Eng. J. 503, 158054. https://doi.org/10.1016/j.cej.2024.158054.

Pullano, S.A., Greco, M., Bianco, M.G., Foti, D., Brunetti, A., Fiorillo, A.S., 2022. Glucose biosensors in clinical practice: principles, limits and perspectives of currently used devices. Theranostics 12, 493–511. https://doi.org/10.7150/thno.64035.

Qiu, S., Xu, Y., Wu, X., Ji, X., 2022. Prussian blue analogues as electrodes for aqueous monovalent ion batteries. Electrochem. Energy Rev. 5, 242–262. https://doi.org/10.1007/s41918-020-00088-x.

Ricci, F., Palleschi, G., 2005. Sensor and biosensor preparation, optimisation and applications of Prussian blue modified electrodes. Biosens. Bioelectron. 21, 389–407. https://doi.org/10.1016/j.bios.2004.12.001.

Schmidt-Speicher, L.M., Länge, K., 2021. Microfluidic integration for electrochemical biosensor applications. Curr. Opin. Electrochem. 29, 100755. https://doi.org/10.1016/j.coelec.2021.100755.

Schubert-Olesen, O., Kröger, J., Siegmund, T., Thurm, U., Halle, M., 2022. Continuous glucose monitoring and physical activity. Int. J. Environ. Res. Publ. Health 19, 12296. https://doi.org/10.3390/ijerph191912296.

Su, X., Hatton, T.A., 2017. Redox-electrodes for selective electrochemical separations. Adv. Colloid Interface Sci., Special Issue in Honor of the 90th Birthday of Prof. Eli Ruckenstein 244, 6–20. https://doi.org/10.1016/j.cis.2016.09.001.

Tang, C., Zhou, K., Wang, R., Li, M., Liu, W., Li, C., Chen, X., Lu, Q., Chang, Y., 2024. Wearable biosensors for human sweat glucose detection based on carbon black nanoparticles. Anal. Bioanal. Chem. 416, 1407–1415. https://doi.org/10.1007/s00216-024-05135-w.

Trojanowicz, M., 2011. Recent developments in electrochemical flow detections—A review: part II. Liquid chromatography. Anal. Chim. Acta 688, 8–35. https://doi.org/10.1016/j.aca.2010.12.024.

Vasylieva, N., Barnych, B., Meiller, A., Maucler, C., Pollegioni, L., Lin, J.-S., Barbier, D., Marinesco, S., 2011. Covalent enzyme immobilization by poly(ethylene glycol) diglycidyl ether (PEGDE) for microelectrode biosensor preparation. Biosens. Bioelectron. 26, 3993–4000. https://doi.org/10.1016/j.bios.2011.03.012.

Welch, E.C., Powell, J.M., Clevinger, T.B., Fairman, A.E., Shukla, A., 2021. Advances in biosensors and diagnostic technologies using nanostructures and nanomaterials. Adv. Funct. Mater. 31, 2104126. https://doi.org/10.1002/adfm.202104126.